Available online at www.sciencedirect.com

ScienceDirect

IFAC PapersOnLine 56-2 (2023) 11173–11178

Optimal Design of Experiments Model Predictive Controller

Zhang Peng Du * **Sandro Kofler** *
Daniel Ritzberger * **Stefan Jakubek** * **Christoph Hametner** **

* *Institute of Mechanics and Mechatronics, TU Wien, Vienna, Austria (e-mail: {zhang.peng.du, sandro.kofler, daniel.ritzberger, stefan.jakubek}@tuwien.ac.at)*
** *Christian Doppler Laboratory for Innovative Control and Monitoring of Automotive Powertrain Systems, TU Wien, Vienna, Austria (e-mail: christoph.hametner@tuwien.ac.at)*

Abstract: System investigations such as simulation, diagnosis, and control require well-identified models. This work proposes an optimal design of experiments model predictive controller (MPC) to obtain experiments for identification. The main contribution is an MPC formulation with a target-oriented implementation of the parameter sensitivity (Fisher information), which remains a convex quadratic problem. Computers can optimally and efficiently solve quadratic problems, including constraints, and the method is demonstrated with a linear cathode model of a polymer electrolyte membrane fuel cell. The MPC is demonstrated in simulations, including disturbances, and significantly improves the parameter identifiability compared to a non-optimized experiment.

Keywords: Experiment design, Identifiability, Input and excitation design, Intelligent control of power systems, Optimal control theory, Optimal operation and control of power systems.

1. INTRODUCTION

A fuel cell (FC) model is generally the basis for many applications, such as simulation, diagnosis, and control. In order to obtain valid analysis conclusions, the models utilized should replicate the dynamic FC behavior quantitatively and qualitatively well. Otherwise, the derived conclusions may be misleading due to erring signal magnitudes and system dynamics. E.g., the simulation shows a sufficient species concentration, but in reality, the FC already experiences fuel starvation, which also affects the degradation diagnosis based on the simulation. Erring system dynamics would highly influence model-based controllers, e.g., according to the model, there is no water condensation, but the real FC is already flooded, devastating the performance without appropriate controller counteractions. Thus, experiments covering the entire operating range with increased parameter sensitivities are required for satisfactory model identification. In this work, a novel optimal design of experiments (DOE) model predictive controller (MPC) based on quadratic programming is introduced, which is a promising method for obtaining well-designed experiments for identification, and it is demonstrated with a simplified cathode model of a polymer electrolyte membrane FC (PEMFC).

The process of obtaining a well-parametrized model is anything but simple. The first question is what model type should be used, and the model types can be roughly categorized into three groups: black-box models, grey-box models, and white-box models, see Jones et al. (2007). Black-box models replicate a system's input and output correlation artificially, white-box models derive their model structure and parameters only from first principles and literature, and grey-box models are a middle ground of both model types. The latter enables a physical interpretation of the model states and parameters, and the models are fitted to real-world systems to replicate their behavior satisfactorily, which is advantageous for diagnosis and control. Thus, grey-box models are often used in FC studies and as well as in this work. The second question is, how should the experiments be designed to get a good base for model identification? DOE can be subdivided into two approaches: non-model-based and model-based. E.g., exciting a system with sequential input steps of arbitrary magnitude and frequency as in Ritzberger et al. (2021) is a non-model-based approach. Another non-model-based approach is to utilize well-established experiments, e.g., a polarization curve experiment for FCs as in the authors' work Du et al. (2021b). However, if system properties are known, this information can be exploited in a target-oriented way. E.g., based on the system dynamics, it can be derived that only excitations in a specific region and frequency range increase the parameter information, and an additional excitation in other regions and frequency ranges barely contribute anything to it. Hence, the experiments can be specifically adapted to a system, leading to fewer and shorter experiments necessary to obtain the same parameter information content as non-specifically designed ones. An often-used measure for parameter information is the Fisher information $\mathcal{I}$ as described in Ljung (1999), which can be analytically derived from a model and an excitation signal. The popularity of the Fisher information is due to the property $\mathrm{Var}(\theta) \geq \mathcal{I}^{-1}$, according to Cramér (1999), which means that the inverse of $\mathcal{I}$ is the

⋆ This project is supported with funds from the Climate and Energy Fund and implemented in line with the "Zero Emission Mobility" programme (grant number 878123).

10.1016/j.ifacol.2023.10.839

lower variance bound of the parameter θ, also known as the Cramér–Rao inequality. Hence, a higher $\mathcal{I}$ means lower parameter uncertainties and the goal is to optimize this measure by designing the experiment appropriately, mainly conducted offline beforehand. E.g., the authors developed an approach where the scalar Fisher information for every parameter is maximized in a steady-state operating point individually, see Du et al. (2023). In Wilson et al. (2014), a trajectory for a two-link cart pendulum is optimized regarding the Fisher information, which is then fed into the real-world system. The online DOE goes further: an MPC optimizes the control input regarding the Fisher information in real-time during operation and considers the actual state and constraints of the system, e.g., as in Jayasankar et al. (2010), where the objective is to find an input to maximize the D-optimality of the sensitivity matrix. In comparison, Larsson et al. (2013) and Marafioti et al. (2014) incorporated the sensitivity matrix as a constraint, demanding it to be bigger than a lower bound to obtain persistent exciting inputs. In most cases, the objective function for DOE MPCs is non-convex and optimized with a numerical solver, which is computationally expensive, and optimality is not guaranteed. Thus, a DOE MPC formulated as a convex quadratic problem is missing, and this would significantly reduce the necessary computational effort and guarantee optimality, which is beneficial for real-time applications.

In order to fill the literature gap, this work presents a novel optimal DOE MPC formulated as a convex problem capable of considering constraints and disturbances. A PEMFC cathode model serves as the linear modeling basis, and an analytical way of evaluating the Fisher information is implemented into the MPC formulation, maintaining the quadratic property, which is the main contribution of this work. This property is achieved by linearly deriving the scalar Fisher information of a single parameter. In this way, it is optimized during operation to increase the parameter sensitivities, and this optimization problem can be optimally and efficiently solved, which is essential for control applications. The MPC simulation study results are presented and thoroughly discussed, and the DOE MPC experiments deliver higher Fisher information than a non-specifically designed one.

The remainder is structured as follows: Section 2 presents the modeling basis and an analytical way of obtaining the Fisher information. The convex MPC formulation considering the Fisher information is presented based on that. Section 3 illustrates the simulation study results of the MPC, including a detailed results discussion.

2. METHODS

This section presents the modeling basis, a simplified control-oriented PEMFC cathode model. Based on this, the analytic Fisher information calculation is shown, which is implemented into a novel convex quadratic DOE MPC formulation, the main contribution of this work. The following holds to keep this work concise: the modeling basis is a linear model with a single input and output, noise is neglected, the model states are always known, and the DOE MPC optimizes for only one parameter. The MPC design is not limited to the shown model and can be extended to multiple inputs, outputs, and parameters. Moreover, the controller can be equally applied to nonlinear models via, e.g., successive linearization as in Zhakatayev et al. (2017).

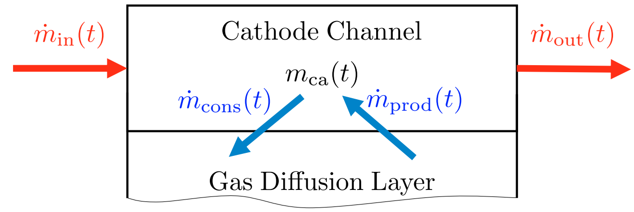

Fig. 1. Sketch of PEMFC cathode model, where $m_{\mathrm{ca}}(t)$ is the mass of the cathode gas, $\dot{m}_{\mathrm{in}}(t)$ is the inflowing air, $\dot{m}_{\mathrm{out}}(t)$ the outflowing mass, $\dot{m}_{\mathrm{cons}}(t)$ the consumed mass, and $\dot{m}_{\mathrm{prod}}(t)$ the produced mass.

2.1 Cathode Model

The modeling basis is a linear control-oriented cathode model of a 30 kW PEMFC stack with 96 cells, a simplified version of Du et al. (2021a). This model was chosen because it keeps the modeling part concise to focus on the MPC part, and it comprises all the necessary properties the authors want to highlight (e.g., a time-constant-like volume parameter), elaborated on later in the results. Simplifying assumptions are made to increase the readability of this work, which do not limit the applicability of the proposed MPC:

(a) The ideal gas law is applicable, and the inflowing mass is dry air, which only consists of nitrogen and oxygen.
(b) The cathode is a lumped volume with no spatial expansions and has only one lumped mass, which considers all the species.
(c) The composition of the cathode mass is equal to the one of dry air at any time, and when there is mass, there is always enough oxygen for consumption.
(d) Influences of the gas diffusion and catalyst layer are neglected except for the mass flows due to the electrochemical reaction.
(e) Diffusion through the membrane is neglected.
(f) The nozzle to the atmosphere behaves linearly, and the cathode is open-ended.
(g) The cathode has a constant uniform temperature.

The mass balance

$$\dot{m}_{\mathrm{ca}}(t)=\dot{m}_{\mathrm{in}}(t)-\dot{m}_{\mathrm{cons}}(t)+\dot{m}_{\mathrm{prod}}(t)-\dot{m}_{\mathrm{out}}(t) \qquad (1)$$

is the cathode's governing ordinary differential equation, and a sketch is given in Fig. 1. In (1), $\dot{m}_{\mathrm{ca}} = \dot{m}_{\mathrm{ca}}(t)$ denotes the time derivative of the lumped cathode gas mass, $\dot{m}_{\mathrm{in}}(t)$ is the inflowing dry air, $\dot{m}_{\mathrm{cons}}(t)$ the consumed mass, $\dot{m}_{\mathrm{prod}}(t)$ the produced mass, and $\dot{m}_{\mathrm{out}}$ the outflowing mass. The right-hand-side variables are defined as follows:

$$\begin{aligned} \dot{m}_{\mathrm{in}}(t)&=\frac{\lambda M_{\mathrm{O_2}} n}{4\mathcal{F} w_{\mathrm{O_2}}} I(t), \quad \dot{m}_{\mathrm{cons}}(t)=\frac{M_{\mathrm{O_2}} n}{4\mathcal{F}} I(t), \\ \dot{m}_{\mathrm{prod}}(t)&=\frac{M_{\mathrm{H_2O}} n}{2\mathcal{F}} I(t), \quad \dot{m}_{\mathrm{out}}(t)=c(p_{\mathrm{ca}}(t)-p_{\mathrm{atm}}). \end{aligned} \qquad (2)$$

The stack current $I = I(t)$ governs the inflowing dry air, consumed, and produced mass. The first mass flow represents a constant stoichiometry λ of oxygen converted to dry air, the second the consumed oxygen, and the third the produced water due to the electrochemical reaction. For the calculation, the following quantities are necessary: the molar mass of oxygen $M_{\mathrm{O_2}}$ and water $M_{\mathrm{H_2O}}$, the number of cells in the stack n, the Faraday constant $\mathcal{F}$, and the oxygen mass fraction in dry air w_{O_2}. A linear nozzle equation governs the outflowing mass, where c is the nozzle coefficient, p_{atm} the atmospheric pressure, and $p_{\mathrm{ca}}(t) = RTm_{\mathrm{ca}}/(VM_{\mathrm{air}})$ is the model output, cathode pressure $p_{\mathrm{ca}} = p_{\mathrm{ca}}(t)$, obtained with the ideal gas law. Here, R is the universal gas constant, T is the uniform cathode temperature, V is the cathode volume, and M_{air} is the molar mass of dry air. The described cathode model has five parameters that are not natural constants: oxygen stoichiometry λ, the number of cells in the stack n, the nozzle coefficient c, the uniform temperature T, and the cathode volume V. The number of cells is known, and the oxygen stoichiometry and the temperature can be manually set. Therefore, only two unknown model parameters $\boldsymbol{\theta} = [\theta_1\ \theta_2]^{\mathrm{T}}$ remain, the nozzle coefficient $\theta_1 = c$ and the cathode volume $\theta_2 = V$. The presented model with the state $x_{\mathrm{m}} = m_{\mathrm{ca}}$, input $u = I$, and output $y = p_{\mathrm{ca}}$ can be rewritten as $\dot{x}_{\mathrm{m}} = f(x_{\mathrm{m}}, u, \boldsymbol{\theta})$ and $y = g(x_{\mathrm{m}}, \boldsymbol{\theta})$. Subsequently, a state-space system is derived for a stationary operating point (denoted by index 0 and $\dot{x}_{\mathrm{m},0} = 0$ holds):

$$\overbrace{\dot{x}_{\mathrm{m}} - \dot{x}_{\mathrm{m},0}}^{\dot{\tilde{x}}_{\mathrm{m}}} = \overbrace{\frac{\partial f(x_{\mathrm{m}}, u, \boldsymbol{\theta})}{\partial x_{\mathrm{m}}}}^{A_{\mathrm{c}}} \overbrace{(x_{\mathrm{m}} - x_{\mathrm{m},0})}^{\tilde{x}_{\mathrm{m}}} + \underbrace{\frac{\partial f(x_{\mathrm{m}}, u, \boldsymbol{\theta})}{\partial u}}_{b_{\mathrm{c}}} \underbrace{(u - u_0)}_{\tilde{u}}, \tag{3a}$$

$$\underbrace{y - y_0}_{\tilde{y}} = \underbrace{\frac{\partial g(x_{\mathrm{m}}, \boldsymbol{\theta})}{\partial x_{\mathrm{m}}}}_{c_{\mathrm{m}}} \underbrace{(x_{\mathrm{m}} - x_{\mathrm{m},0})}_{\tilde{x}_{\mathrm{m}}}. \tag{3b}$$

The system A_{c}, input b_{c}, and output coefficient c_{m} are partial model derivatives, the indices c and m denote time-continuous and model, respectively, and a tilde indicates deviation from the operating point. In this form, the model is applicable in the following derivations.

2.2 Analytical Fisher Information Derivation

In order to optimize the identifiability of an unknown parameter, e.g., the volume V, the sensitivity measure Fisher information is used, where the inverse is the lower parameter variance bound, so higher information for V means lower uncertainties during identification. In order to calculate the Fisher information, a first plausible guess of the unknown parameter is essential, which can be derived from literature and expert knowledge, e.g., the nominal volume according to the datasheet. For readability reasons, the DOE MPC only optimizes the sensitivity of one parameter. However, the procedure is extendable for multiple parameters. For the Fisher information, the state parameter sensitivity $\tilde{\xi}_i = \mathrm{d}\tilde{x}_{\mathrm{m}}/\mathrm{d}\theta_i$ and output parameter sensitivity $\tilde{\psi}_i = \mathrm{d}\tilde{y}/\mathrm{d}\theta_i$ are required, which are obtained by calculating the total derivative of the given state-space model (3) with respect to a parameter θ_i as in Řehoř and Havlena (2014):

$$\frac{\mathrm{d}}{\mathrm{d}t}\tilde{\xi}_i = \frac{\mathrm{d}}{\mathrm{d}t}\left(\frac{\mathrm{d}}{\mathrm{d}\theta_i}\tilde{x}_{\mathrm{m}}\right) = \frac{\mathrm{d}}{\mathrm{d}\theta_i}\left(\frac{\mathrm{d}}{\mathrm{d}t}\tilde{x}_{\mathrm{m}}\right) = \frac{\mathrm{d}}{\mathrm{d}\theta_i}(A_{\mathrm{c}}\tilde{x}_{\mathrm{m}} + b_{\mathrm{c}}\tilde{u}) = A_{\mathrm{c},\theta_i}\tilde{x}_{\mathrm{m}} + A_{\mathrm{c}}\tilde{\xi}_i + b_{\mathrm{c},\theta_i}\tilde{u}, \tag{4a}$$

$$\tilde{\psi}_i = \frac{\mathrm{d}}{\mathrm{d}\theta_i}(c_{\mathrm{m}}\tilde{x}_{\mathrm{m}}) = c_{\mathrm{m},\theta_i}\tilde{x}_{\mathrm{m}} + c_{\mathrm{m}}\tilde{\xi}_i. \tag{4b}$$

The variables with θ_i in the index denote the partial derivative of the original variable with respect to the parameter in the index. The solution of (4) delivers the time-continuous output parameter sensitivity $\psi_i = \tilde{\psi}_i + \psi_{i,0}$, and for the evaluation of the Fisher information $\mathcal{I}$, only the sampled (at the time instants t_k for $k \in \{1,2,\ldots,N\}$) counterpart $\psi_{i,k}$ is relevant. The reason is that a measured output signal, i.e., cathode pressure, is unknown between the sampling instants, and the unknown parts do not contribute any information. Finally, $\mathcal{I}$ is calculated utilizing the absolute output parameter sensitivity as in Ljung (1999)

$$\mathcal{I} = \sum_{k=1}^{N} \psi_{i,k} \frac{1}{\sigma^2} \psi_{i,k}. \tag{5}$$

Here, N is the total number of samples, and σ^2 represents the prediction error variance, which is the measurement noise variance under the assumption of a perfect model. The Fisher information is a square matrix with an order equivalent to the number of parameters, and in this work, it is only a scalar because only one parameter is considered. Moreover, whether a parameter is (uniquely) identifiable could have two reasons: either the experiment is not exciting the specific parameter (e.g., phase change coefficient and the experiment does not consider an appropriate operating region), or due to the model structure (e.g., the diffusion through the membrane is governed by two linearly interdependent parameters). This derivation already forms the prerequisite for the following implementation in the MPC.

2.3 Optimal Design of Experiments Controller Design

An MPC is a controller where the resulting system input, i.e., stack current, is calculated online at every sampling instant by solving a finite horizon optimal control problem. The initial state is the system state at the moment, i.e., the cathode gas mass, and the optimization delivers a finite control trajectory, where the first control action is applied to the system. Please refer to Wang (2009) for a detailed description of MPCs. The main contribution of this work is an optimal DOE MPC, which optimizes the system input regarding the Fisher information while tracking a reference, considering constraints, disturbances, and the actual system state. Constraints are, e.g., the rate of current change and feasible regions for the cathode pressure, and the Fisher information is implemented into the MPC formulation while maintaining the convex problem property, the highlight of this work. In order to design the controller, the state-space (3) and sensitivity model (4) need to be discretized in time as described in Řehoř and Havlena (2014):

$$\begin{bmatrix} A_{\mathrm{d}} & 0 & b_{\mathrm{d}} \\ A_{\mathrm{d},\theta_i} & A_{\mathrm{d}} & b_{\mathrm{d},\theta_i} \\ 0 & 0 & 1 \end{bmatrix} = \exp\left(\begin{bmatrix} A_{\mathrm{c}} & 0 & b_{\mathrm{c}} \\ A_{\mathrm{c},\theta_i} & A_{\mathrm{c}} & b_{\mathrm{c},\theta_i} \\ 0 & 0 & 0 \end{bmatrix} \Delta t\right). \tag{6}$$

For the discretization, the constant sampling time Δt is required (set to 0.1 s), and the index d denotes discrete. The discrete versions of (3) and (4) are given as

$$\tilde{x}_{\mathrm{m},k+1} = A_{\mathrm{d}}\tilde{x}_{\mathrm{m},k} + b_{\mathrm{d}}\tilde{u}_k, \tag{7a}$$

$$\tilde{y}_{k+1} = c_{\mathrm{m}}\tilde{x}_{\mathrm{m},k+1}, \tag{7b}$$

$$\tilde{\xi}_{i,k+1} = A_{\mathrm{d},\theta_i}\tilde{x}_{\mathrm{m},k} + A_{\mathrm{d}}\tilde{\xi}_{i,k} + b_{\mathrm{d},\theta_i}\tilde{u}_k, \tag{7c}$$

$$\tilde{\psi}_{i,k+1} = c_{\mathrm{m},\theta_i}\tilde{x}_{\mathrm{m},k+1} + c_{\mathrm{m}}\tilde{\xi}_{i,k+1}, \tag{7d}$$

with the discretized system variables. In addition, the incremental (denoted by Δ) formulation as in Wang (2009),

$$\overbrace{\tilde{x}_{\mathrm{m},k+1}-\tilde{x}_{\mathrm{m},k}}^{\Delta\tilde{x}_{\mathrm{m},k+1}}=A_{\mathrm{d}}\overbrace{(\tilde{x}_{\mathrm{m},k}-\tilde{x}_{\mathrm{m},k-1})}^{\Delta\tilde{x}_{\mathrm{m},k}}+b_{\mathrm{d}}\overbrace{(\tilde{u}_k-\tilde{u}_{k-1})}^{\Delta\tilde{u}_k}, \tag{8a}$$

$$\underbrace{\tilde{y}_{k+1}-\tilde{y}_k}_{\Delta\tilde{y}_{k+1}}=c_{\mathrm{m}}\underbrace{(\tilde{x}_{\mathrm{m},k+1}-\tilde{x}_{\mathrm{m},k})}_{\Delta\tilde{x}_{\mathrm{m},k+1}}, \tag{8b}$$

of the discrete cathode model leads to an augmented system

$$\overbrace{\begin{bmatrix}\Delta\tilde{x}_{\mathrm{m},k+1}\\ \tilde{y}_{k+1}\end{bmatrix}}^{\boldsymbol{x}_{\mathrm{R},k+1}}=\overbrace{\begin{bmatrix}A_{\mathrm{d}} & 0\\ c_{\mathrm{m}}A_{\mathrm{d}} & 1\end{bmatrix}}^{\boldsymbol{A}_{\mathrm{R}}}\overbrace{\begin{bmatrix}\Delta\tilde{x}_{\mathrm{m},k}\\ \tilde{y}_k\end{bmatrix}}^{\boldsymbol{x}_{\mathrm{R},k}}+\overbrace{\begin{bmatrix}b_{\mathrm{d}}\\ c_{\mathrm{m}}b_{\mathrm{d}}\end{bmatrix}}^{\boldsymbol{b}_{\mathrm{R}}}\Delta\tilde{u}_k, \tag{9a}$$

$$\tilde{y}_{k+1}=\underbrace{[0\ 1]}_{\boldsymbol{c}_{\mathrm{R}}^{\mathrm{T}}}\underbrace{\begin{bmatrix}\Delta\tilde{x}_{\mathrm{m},k+1}\\ \tilde{y}_{k+1}\end{bmatrix}}_{\boldsymbol{x}_{\mathrm{R},k+1}}, \tag{9b}$$

which is used for the MPC design. The index R denotes reference tracking, elaborated on later. Using the augmented system, the future output trajectory, i.e., cathode pressure, at instant k of the system is calculated, dependent on the to-be-optimized system input, i.e., stack current, with

$$\begin{aligned}\boldsymbol{x}_{\mathrm{R},k+1|k}&=\boldsymbol{A}_{\mathrm{R}}\boldsymbol{x}_{\mathrm{R},k}+\boldsymbol{b}_{\mathrm{R}}\Delta\tilde{u}_k,\\ \boldsymbol{x}_{\mathrm{R},k+2|k}&=\boldsymbol{A}_{\mathrm{R}}\boldsymbol{x}_{\mathrm{R},k+1|k}+\boldsymbol{b}_{\mathrm{R}}\Delta\tilde{u}_{k+1},\\ &=\boldsymbol{A}_{\mathrm{R}}(\boldsymbol{A}_{\mathrm{R}}\boldsymbol{x}_{\mathrm{R},k}+\boldsymbol{b}_{\mathrm{R}}\Delta\tilde{u}_k)+\boldsymbol{b}_{\mathrm{R}}\Delta\tilde{u}_{k+1},\\ &\ \ \vdots\\ \boldsymbol{x}_{\mathrm{R},k+N|k}&=\boldsymbol{A}_{\mathrm{R}}^N\boldsymbol{x}_{\mathrm{R},k}+\boldsymbol{A}_{\mathrm{R}}^{N-1}\boldsymbol{b}_{\mathrm{R}}\Delta\tilde{u}_k\\ &\quad+\boldsymbol{A}_{\mathrm{R}}^{N-2}\boldsymbol{b}_{\mathrm{R}}\Delta\tilde{u}_{k+1}+\dots+\boldsymbol{b}_{\mathrm{R}}\Delta\tilde{u}_{k+N-1},\end{aligned} \tag{10a}$$

$$\begin{aligned}\tilde{y}_{k+1|k}&=\boldsymbol{c}_{\mathrm{R}}^{\mathrm{T}}\boldsymbol{x}_{\mathrm{R},k+1}=\boldsymbol{c}_{\mathrm{R}}^{\mathrm{T}}(\boldsymbol{A}_{\mathrm{R}}\boldsymbol{x}_{\mathrm{R},k}+\boldsymbol{b}_{\mathrm{R}}\Delta\tilde{u}_k),\\ \tilde{y}_{k+2|k}&=\boldsymbol{c}_{\mathrm{R}}^{\mathrm{T}}(\boldsymbol{A}_{\mathrm{R}}^2\boldsymbol{x}_{\mathrm{R},k}+\boldsymbol{A}_{\mathrm{R}}\boldsymbol{b}_{\mathrm{R}}\Delta\tilde{u}_k+\boldsymbol{b}_{\mathrm{R}}\Delta\tilde{u}_{k+1}),\\ &\ \ \vdots\\ \tilde{y}_{k+N|k}&=\boldsymbol{c}_{\mathrm{R}}^{\mathrm{T}}(\boldsymbol{A}_{\mathrm{R}}^N\boldsymbol{x}_{\mathrm{R},k}+\boldsymbol{A}_{\mathrm{R}}^{N-1}\boldsymbol{b}_{\mathrm{R}}\Delta\tilde{u}_k\\ &\quad+\boldsymbol{A}_{\mathrm{R}}^{N-2}\boldsymbol{b}_{\mathrm{R}}\Delta\tilde{u}_{k+1}+\dots+\boldsymbol{b}_{\mathrm{R}}\Delta\tilde{u}_{k+N-1}).\end{aligned} \tag{10b}$$

Here, N denotes the prediction horizon (set to 50), which is the number of prediction samples, and the control horizon, the number of manipulable input samples, is identical to the former to increase the readability. With the vectors

$$\boldsymbol{Y}_{\mathrm{R}}=[\tilde{y}_{k+1|k}\ \tilde{y}_{k+2|k}\ \dots\ \tilde{y}_{k+N|k}]^{\mathrm{T}}, \tag{11a}$$

$$\Delta\boldsymbol{U}=[\Delta\tilde{u}_k\ \Delta\tilde{u}_{k+1}\ \dots\ \Delta\tilde{u}_{k+N-1}]^{\mathrm{T}}, \tag{11b}$$

the predictions (10) can be rewritten as

$$\boldsymbol{Y}_{\mathrm{R}}=\boldsymbol{F}_{\mathrm{R}}\boldsymbol{x}_{\mathrm{R},k}+\boldsymbol{\Phi}_{\mathrm{R}}\Delta\boldsymbol{U}, \tag{12}$$

with the relations

$$\boldsymbol{F}_{\mathrm{R}}=\begin{bmatrix}\boldsymbol{c}_{\mathrm{R}}^{\mathrm{T}}\boldsymbol{A}_{\mathrm{R}}\\ \boldsymbol{c}_{\mathrm{R}}^{\mathrm{T}}\boldsymbol{A}_{\mathrm{R}}^2\\ \vdots\\ \boldsymbol{c}_{\mathrm{R}}^{\mathrm{T}}\boldsymbol{A}_{\mathrm{R}}^N\end{bmatrix}, \tag{13a}$$

$$\boldsymbol{\Phi}_{\mathrm{R}}=\begin{bmatrix}\boldsymbol{c}_{\mathrm{R}}^{\mathrm{T}}\boldsymbol{b}_{\mathrm{R}} & 0 & \dots & 0\\ \boldsymbol{c}_{\mathrm{R}}^{\mathrm{T}}\boldsymbol{A}_{\mathrm{R}}\boldsymbol{b}_{\mathrm{R}} & \boldsymbol{c}_{\mathrm{R}}^{\mathrm{T}}\boldsymbol{b}_{\mathrm{R}} & \dots & 0\\ \vdots & \vdots & \ddots & \vdots\\ \boldsymbol{c}_{\mathrm{R}}^{\mathrm{T}}\boldsymbol{A}_{\mathrm{R}}^{N-1}\boldsymbol{b}_{\mathrm{R}} & \boldsymbol{c}_{\mathrm{R}}^{\mathrm{T}}\boldsymbol{A}_{\mathrm{R}}^{N-2}\boldsymbol{b}_{\mathrm{R}} & \dots & \boldsymbol{c}_{\mathrm{R}}^{\mathrm{T}}\boldsymbol{b}_{\mathrm{R}}\end{bmatrix}. \tag{13b}$$

The same procedure is repeated to obtain the predicted parameter sensitivities with the augmented model based on Řehoř and Havlena (2014):

$$\begin{aligned}\overbrace{\begin{bmatrix}\Delta\tilde{x}_{\mathrm{m},k+1}\\ \Delta\tilde{\xi}_{i,k+1}\\ \tilde{\psi}_{i,k+1}\end{bmatrix}}^{\boldsymbol{x}_{\mathcal{I},k+1}}&=\overbrace{\begin{bmatrix}A_{\mathrm{d}} & 0 & 0\\ A_{\mathrm{d},\theta_i} & A_{\mathrm{d}} & 0\\ c_{\mathrm{m},\theta_i}A_{\mathrm{d}}+c_{\mathrm{m}}A_{\mathrm{d},\theta_i} & c_{\mathrm{m}}A_{\mathrm{d}} & 1\end{bmatrix}}^{\boldsymbol{A}_{\mathcal{I}}}\\ &\cdot\overbrace{\begin{bmatrix}\Delta\tilde{x}_{\mathrm{m},k}\\ \Delta\tilde{\xi}_{i,k}\\ \tilde{\psi}_{i,k}\end{bmatrix}}^{\boldsymbol{x}_{\mathcal{I},k}}+\overbrace{\begin{bmatrix}b_{\mathrm{d}}\\ b_{\mathrm{d},\theta_i}\\ c_{\mathrm{m},\theta_i}b_{\mathrm{d}}+c_{\mathrm{m}}b_{\mathrm{d},\theta_i}\end{bmatrix}}^{\boldsymbol{b}_{\mathcal{I}}}\Delta\tilde{u}_k,\end{aligned} \tag{14a}$$

$$\psi_{i,k+1}=\underbrace{[0\ 0\ 1]}_{\boldsymbol{c}_{\mathcal{I}}^{\mathrm{T}}}\underbrace{\begin{bmatrix}\Delta\tilde{x}_{\mathrm{m},k+1}\\ \Delta\tilde{\xi}_{i,k+1}\\ \tilde{\psi}_{i,k+1}\end{bmatrix}}_{\boldsymbol{x}_{\mathcal{I},k+1}}+\psi_{i,0}, \tag{14b}$$

resulting in

$$\boldsymbol{Y}_{\mathcal{I}}=\boldsymbol{F}_{\mathcal{I}}\boldsymbol{x}_{\mathcal{I},k}+\boldsymbol{\Phi}_{\mathcal{I}}\Delta\boldsymbol{U}+\mathbb{I}\psi_{i,0}. \tag{15}$$

Here, $\mathbb{I}$ is a column vector with ones in every entry. The output sensitivity $\psi_{i,0}$ at the operating point must also be considered because it contains information, e.g., the operating point pressure (model output y, so ψ_i, too) depends on the unknown nozzle coefficient. Note that the exact relation

$$\mathcal{I}=\sum_{k=1}^{N}\psi_{i,k}\frac{1}{\sigma^2}\psi_{i,k}=\boldsymbol{Y}_{\mathcal{I}}^{\mathrm{T}}\boldsymbol{Y}_{\mathcal{I}}/\sigma^2 \tag{16}$$

for the Fisher information (5) holds, enabling its prediction calculation. In order to minimize the parameter uncertainties for the volume or nozzle coefficient, $\mathcal{I}^{-1}$ should be minimized, which is equivalent to maximizing $\mathcal{I}$. With the available predictions, the MPC objective function is given as

$$\begin{aligned}J(\Delta\boldsymbol{U})=&\overbrace{(\boldsymbol{Y}_{\mathrm{R,ref}}-\boldsymbol{Y}_{\mathrm{R}})^{\mathrm{T}}\boldsymbol{Q}_{\mathrm{R}}(\boldsymbol{Y}_{\mathrm{R,ref}}-\boldsymbol{Y}_{\mathrm{R}})}^{\text{Reference tracking}}\\ &+\underbrace{\Delta\boldsymbol{U}^{\mathrm{T}}\boldsymbol{R}\Delta\boldsymbol{U}}_{\text{Input penalty}}-\underbrace{Q_{\mathcal{I}}\boldsymbol{Y}_{\mathcal{I}}^{\mathrm{T}}\boldsymbol{Y}_{\mathcal{I}}}_{\text{Fisher information}},\end{aligned} \tag{17}$$

where $\boldsymbol{Y}_{\mathrm{R,ref}}$ is the output reference, $\boldsymbol{Q}_{\mathrm{R}}\succeq 0$ the output deviation weighting, $\boldsymbol{R}\succ 0$ the input weighting, and $Q_{\mathcal{I}}=q_{\mathcal{I}}/\sigma^2\geq 0$ combines the weighting for the Fisher information $q_{\mathcal{I}}$ and its measurement noise variance σ^2. An MPC problem is usually minimized, so subtracting the Fisher information in J is equivalent to maximizing $\mathcal{I}$. The objective function (17) is simplified using an augmented model combining (9) and (14):

$$\begin{aligned}\overbrace{\begin{bmatrix}\Delta\tilde{x}_{\mathrm{m},k+1}\\ \Delta\tilde{\xi}_{i,k+1}\\ \tilde{y}_{k+1}\\ \tilde{\psi}_{i,k+1}\end{bmatrix}}^{\boldsymbol{x}_{k+1}}&=\overbrace{\begin{bmatrix}A_{\mathrm{d}} & 0 & 0 & 0\\ A_{\mathrm{d},\theta_i} & A_{\mathrm{d}} & 0 & 0\\ c_{\mathrm{m}}A_{\mathrm{d}} & 0 & 1 & 0\\ c_{\mathrm{m},\theta_i}A_{\mathrm{d}}+c_{\mathrm{m}}A_{\mathrm{d},\theta_i} & c_{\mathrm{m}}A_{\mathrm{d}} & 0 & 1\end{bmatrix}}^{\boldsymbol{A}}\\ &\cdot\overbrace{\begin{bmatrix}\Delta\tilde{x}_{\mathrm{m},k}\\ \Delta\tilde{\xi}_{i,k}\\ \tilde{y}_k\\ \tilde{\psi}_{i,k}\end{bmatrix}}^{\boldsymbol{x}_k}+\overbrace{\begin{bmatrix}b_{\mathrm{d}}\\ b_{\mathrm{d},\theta_i}\\ c_{\mathrm{m}}b_{\mathrm{d}}\\ c_{\mathrm{m},\theta_i}b_{\mathrm{d}}+c_{\mathrm{m}}b_{\mathrm{d},\theta_i}\end{bmatrix}}^{\boldsymbol{b}}\Delta\tilde{u}_k,\end{aligned} \tag{18a}$$

$$\underbrace{\begin{bmatrix}\tilde{y}_{k+1}\\ \tilde{\psi}_{i,k+1}\end{bmatrix}}_{\boldsymbol{y}_{k+1}}=\underbrace{\begin{bmatrix}0 & 0 & 1 & 0\\ 0 & 0 & 0 & 1\end{bmatrix}}_{\boldsymbol{C}}\underbrace{\begin{bmatrix}\Delta\tilde{x}_{\mathrm{m},k+1}\\ \Delta\tilde{\xi}_{i,k+1}\\ \tilde{y}_{k+1}\\ \tilde{\psi}_{i,k+1}\end{bmatrix}}_{\boldsymbol{x}_{k+1}}+\underbrace{\begin{bmatrix}0\\ 1\end{bmatrix}}_{\boldsymbol{c}_{\psi}}\psi_{i,0}. \tag{18b}$$

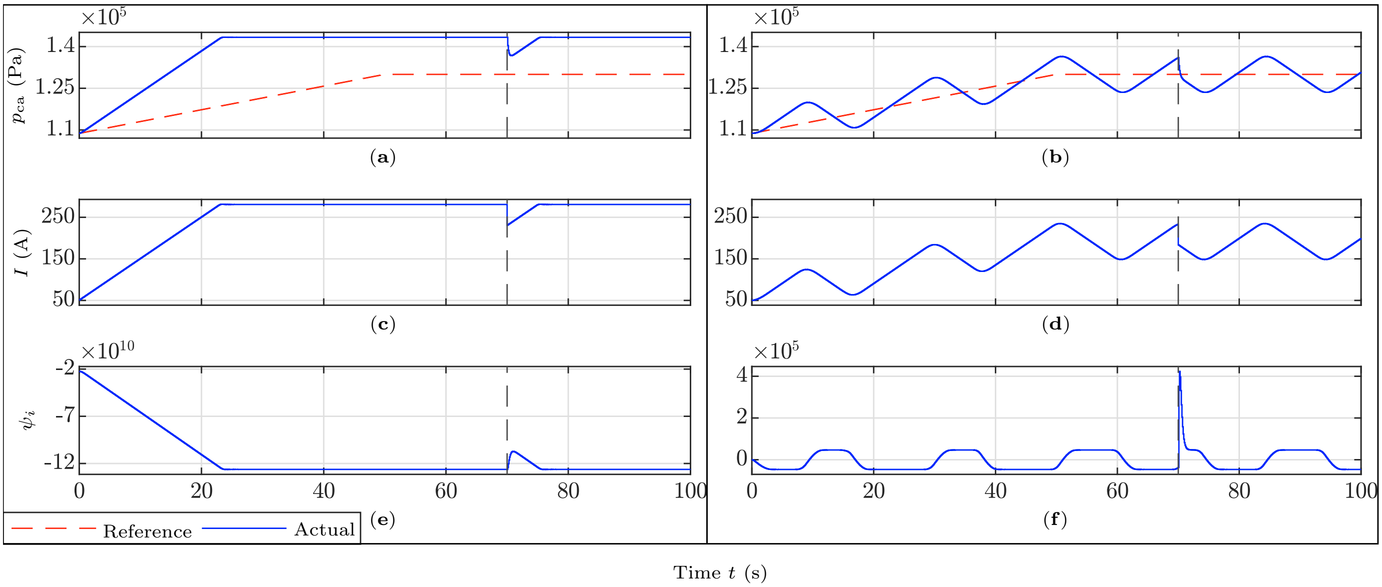

Fig. 2. Simulation results of the DOE MPC are illustrated. The left column shows the optimized results for the nozzle coefficient c, and the right one shows the volume V results. The top panel depicts the model output cathode pressure p_{ca}, the middle one the model input stack current I, and the bottom one the respective output parameter sensitivity ψ_i. The blue lines visualize the model's actual behavior, the red ones the corresponding references, and the black dashed lines indicate the start of the step disturbance.

The already shown prediction approach is applied for the combined augmented model and results in

$$\boldsymbol{Y} = \boldsymbol{F}\boldsymbol{x} + \boldsymbol{\Phi}\Delta\boldsymbol{U} + \bar{\boldsymbol{c}}_{\psi}\psi_{i,0}, \tag{19}$$

with the vectors

$$\boldsymbol{Y} = [\boldsymbol{y}_{k+1|k}\ \boldsymbol{y}_{k+2|k}\ \dots\ \boldsymbol{y}_{k+N|k}]^{\mathrm{T}}, \tag{20a}$$

$$\bar{\boldsymbol{c}}_{\psi} = [\boldsymbol{c}_{\psi}\ \boldsymbol{c}_{\psi}\ \dots\ \boldsymbol{c}_{\psi}]^{\mathrm{T}}. \tag{20b}$$

Finally, the quadratic MPC objective function is given in the well-known form:

$$J(\Delta\boldsymbol{U}) = (\boldsymbol{Y}_{\mathrm{ref}} - \boldsymbol{Y})^{\mathrm{T}}\boldsymbol{Q}(\boldsymbol{Y}_{\mathrm{ref}} - \boldsymbol{Y}) + \Delta\boldsymbol{U}^{\mathrm{T}}\boldsymbol{R}\Delta\boldsymbol{U}, \tag{21}$$

where $\boldsymbol{Q}$ is the weighting matrix considering the weights for the $\tilde{y}$ and ψ_i correspondingly. The minus in (17) for the Fisher information is merged with the weights in $\boldsymbol{Q}$, and the reference in $\boldsymbol{Y}_{\mathrm{ref}}$ for ψ_i is zero, so (17) and (21) are equivalent. Note that the Hessian matrix of (21) is $(\boldsymbol{\Phi}^{\mathrm{T}}\boldsymbol{Q}\boldsymbol{\Phi} + \boldsymbol{R})$, which has to be positive-definite to obtain the global minimum. This property is not automatically fulfilled due to the negative weights for the ψ_i in $\boldsymbol{Q}$. Positive definiteness can be enforced by, e.g., choosing an appropriate $\boldsymbol{R} = \boldsymbol{E}r$, where $\boldsymbol{E}$ is the identity matrix, and $r > 0$ is a proper scalar. Note that $\boldsymbol{R}$ penalizes the incremental input and not the absolute one, and of course, increasing it is conflictive with optimizing the parameter identifiability, the initial goal. So, a trade-off needs to be found, and a meaningful way of choosing r is to set it at the lowest possible value so that the Hessian matrix is just positive definite. By doing so, the excitation penalization is minimal by maintaining the convex property of the programming problem, given as follows:

$$\begin{aligned} &\Delta\boldsymbol{U}_{\mathrm{opt}} = \arg\min_{\Delta\boldsymbol{U}} J(\Delta\boldsymbol{U}) \\ &\text{with respect to} \\ &\left.\begin{aligned} \Delta\tilde{u}_{\min} \le \Delta\tilde{u}_l \le \Delta\tilde{u}_{\max} \\ \tilde{u}_{\min} \le \tilde{u}_l \le \tilde{u}_{\max} \end{aligned}\right\} \text{ for } l \in \{k, k+1, \dots, k+N-1\} \\ &\tilde{y}_{\min} \le \tilde{y}_l \le \tilde{y}_{\max} \text{ for } l \in \{k+1, k+2, \dots, k+N\} \end{aligned} \tag{22}$$

By adjusting the ratio of the weights in $\boldsymbol{Q}$, the MPC behaves more like a reference follower or tries to increase the parameter identifiability, respectively. A controller usually stabilizes a system, but to increase the identifiability, it tends to destabilize a system if no constraints are considered. Thus, constraints are mandatory because otherwise, the MPC excites the system too aggressively, leading to instability and physical damage. E.g., an unconstrained problem would lead to too high current amplitudes and frequencies, harming the system. Thus, the constraints for the system with $u_0 = 50\mathrm{A}$ and $y_0 = 109\mathrm{kPa}$ are set to

$$\Delta\tilde{u}_{\min} = -10\tfrac{\mathrm{A}}{\mathrm{s}}\Delta t, \qquad \Delta\tilde{u}_{\max} = 10\tfrac{\mathrm{A}}{\mathrm{s}}\Delta t, \tag{23a}$$

$$\tilde{u}_{\min} = 0\mathrm{A}, \qquad \tilde{u}_{\max} = 350\mathrm{A}, \tag{23b}$$

$$\tilde{y}_{\min} = -7.48\mathrm{kPa}, \qquad \tilde{y}_{\max} = 51.2\mathrm{kPa}. \tag{23c}$$

To implement the constraints and, if required, slack variables into the problem, please refer to Wang (2009). Regarding closed-loop stability, the optimization problem (22) could be extended with terminal set constraints and a terminal cost, where the weightings for the sensitivities ψ_i are zero after the prediction horizon. Thus, the calculation of the terminal cost reduces to one for a regular reference tracking MPC. These extensions are out of this work's scope, and the reader is referred to Rawlings et al. (2019) in this regard.

3. RESULTS AND DISCUSSION

The simulation results of the proposed DOE MPC are shown in Fig. 2. The results optimized for the nozzle coefficient are in the left column, and the ones for the volume are in the right. In the nozzle coefficient case, the MPC increases the input (Fig. 2c) to obtain a higher pressure by accepting more deviations from the reference (Fig. 2a). Under consideration of the objective function, it tries to maximize the difference between the cathode pressure and the environment because, in this case, the nozzle coefficient is most identifiable, see (2) and Fig. 2e. The MPC behaves entirely differ-

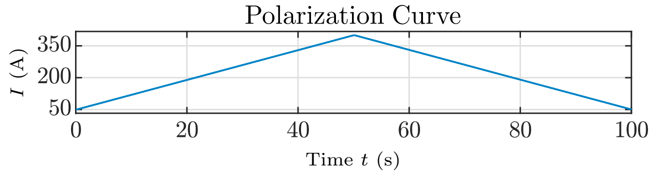

Fig. 3. The shown current excitation I of a polarization curve experiment covers the whole operating range.

ently for the volume because the latter behaves like a time constant. As a result, it is only identifiable during transients, which can be seen in Fig. 2f around the places where the rate of change for the current is zero, and as a consequence, the output parameter sensitivity is zero too. Thus, the MPC enforces an oscillating input trajectory (Fig. 2d) and system behavior while following the reference (Fig. 2b) and considering the constraints. There are always control errors in the real world, e.g., due to model mismatch and disturbances. An advantage of the MPC is that it notices and reacts accordingly. An input disturbance ($-50\,\mathrm{A}$ current step, e.g., an uncontrollable auxiliary load dropped) is applied at $t = 70\mathrm{s}$, and the MPC plays its advantage and counteracts by adjusting the stack current. A polarization curve excitation is shown in Fig. 3, and its Fisher information is evaluated to benchmark the MPC's performance. The DOE MPC yields for the nozzle coefficient (Fig. 2e) a 10.3 % higher Fisher information, and for the volume (Fig. 2f), a 132 % higher one than for the polarization curve experiment while tracking a reference, leading to lower uncertainties in the identification. Note that all the experiments have the same length, meaning that the DOE MPC would require shorter (and fewer) experiments to achieve the same identification result as non-specifically optimized ones. Optimized experiments from the proposed DOE MPC yield better-parametrized models, which are the base for further applications such as simulation, diagnosis, and control.

4. CONCLUSION

A well-identified model is a basis for further applications. This work proposes a novel optimal DOE MPC considering constraints and guaranteeing optimality to contribute to the identification challenge. Based on a PEMFC cathode, the linear modeling basis, a classic MPC formulation is defined for a single input, output, and parameter. In addition, the Fisher information evaluation is analytically derived and implemented into the MPC objective function, which stays a convex quadratic problem. The latter can be efficiently solved, and the optimal solution can be evaluated. The MPC results are shown and discussed for two parameters individually, including disturbances. Finally, a significant increase in Fisher information is shown compared to a commonly-used polarization curve experiment.

Future work incorporates the extension of the MPC to multiple inputs, outputs, and parameters, including nonlinear models and direct feedthrough behavior. The main task is to find a well-defined objective function because the Fisher information is a matrix in the multiple-parameter case, which needs to be considered via an optimality criterion, and the challenge here is to keep the convex problem property. Another research direction could be investigating meaningful ways to consider the Fisher information via constraints by maintaining a relatively simple optimization problem. Moreover, the MPC's stability properties and experimental validation are additional research directions.

REFERENCES

Cramér, H. (1999). *Mathematical Methods of Statistics*, volume 9. Princeton University Press, Princeton, NJ, USA.

Du, Z.P., Kravos, A., Steindl, C., Katrašnik, T., Jakubek, S., and Hametner, C. (2021a). Physically Motivated Water Modeling in Control-Oriented Polymer Electrolyte Membrane Fuel Cell Stack Models. *Energies*, 14(22), 7693.

Du, Z.P., Steindl, C., and Jakubek, S. (2021b). Efficient Two-Step Parametrization of a Control-Oriented Zero-Dimensional Polymer Electrolyte Membrane Fuel Cell Model Based on Measured Stack Data. *Processes*, 9(4), 713.

Du, Z.P., Steindl, C., Jakubek, S., and Hametner, C. (2023). Concentration Estimation for Fuel Cells: Design of Experiments, Nonlinear Identification, and Observer Design With Experimental Validation. *IEEE Access*, 11, 10453–10470.

Jayasankar, B.R., Huang, B., and Ben-Zvi, A. (2010). Receding horizon experiment design with application in SOFC parameter estimation. *IFAC Proc. Vol.*, 43(5), 541–546.

Jones, D.M., Watton, J., and Brown, K.J. (2007). Comparison of black-, white-, and grey-box models to predict ultimate tensile strength of high-strength hot rolled coils at the Port Talbot hot strip mill. *Proc. Inst. Mech. Eng. Part L J. Mater. Des. Appl.*, 221(1), 1–9.

Larsson, C.A., Annergren, M., Hjalmarsson, H., Rojas, C.R., Bombois, X., Mesbah, A., and Moden, P.E. (2013). Model predictive control with integrated experiment design for output error systems. In *2013 European Control Conference (ECC)*, 3790–3795. IEEE.

Ljung, L. (1999). Parameter Estimation Methods. In *System Identification: Theory for the User*, 169–207. Prentice Hall PTR, Englewood Cliffs, NJ, USA, 2nd edition.

Marafioti, G., Bitmead, R.R., and Hovd, M. (2014). Persistently exciting model predictive control. *Int. J. Adapt. Control Signal Process.*, 28(6), 536–552.

Rawlings, J.B., Mayne, D.Q., and Diehl, M.M. (2019). *Model Predictive Control: Theory, Computation, and Design.* Nob Hill Publishing, Santa Barbara, CA, USA.

Ritzberger, D., Höflinger, J., Du, Z.P., Hametner, C., and Jakubek, S. (2021). Data-driven parameterization of polymer electrolyte membrane fuel cell models via simultaneous local linear structured state space identification. *Int. J. Hydrogen Energy*, 46(21), 11878–11893.

Wang, L. (2009). *Model Predictive Control System Design and Implementation Using MATLAB.* Advances in Industrial Control. Springer London, London, UK.

Wilson, A.D., Schultz, J.A., and Murphey, T.D. (2014). Trajectory Synthesis for Fisher Information Maximization. *IEEE Trans. Robot.*, 30(6), 1358–1370.

Zhakatayev, A., Rakhim, B., Adiyatov, O., Baimyshev, A., and Varol, H.A. (2017). Successive linearization based model predictive control of variable stiffness actuated robots. In *2017 IEEE International Conference on Advanced Intelligent Mechatronics (AIM)*, 1774–1779. IEEE, New York, NY, USA.

Řehoř, J. and Havlena, V. (2014). Maximum Likelihood Estimation of LTI Continuous-Time Grey-box Models. *IFAC Proc. Vol.*, 47(3), 3739–3744.